




Self-healing solitonic slip pulses in frictional systems


Anna Pomyalov,^{1,*} Yuri Lubomirsky,^{1,*} Lara Braverman ^{1,2} Efim A. Brener ^{3,4} and Eran Bouchbinder ^{1,†}

¹*Chemical and Biological Physics Department, Weizmann Institute of Science, Rehovot 7610001, Israel*

²*Department of Physics, The University of Chicago, Chicago, Illinois 60637, USA*

³*Peter Grünberg Institut, Forschungszentrum Jülich, D-52425 Jülich, Germany*

⁴*Institute for Energy and Climate Research, Forschungszentrum Jülich, D-52425 Jülich, Germany*

 (Received 30 May 2022; revised 22 August 2022; accepted 9 December 2022; published 3 January 2023)

A prominent spatiotemporal failure mode of frictional systems is self-healing slip pulses, which are propagating solitonic structures that feature a characteristic length. Here, we numerically derive a family of steady state slip pulse solutions along generic and realistic rate-and-state dependent frictional interfaces, separating large deformable bodies in contact. Such nonlinear interfaces feature a nonmonotonic frictional strength as a function of the slip velocity, with a local minimum. The solutions exhibit a diverging length and strongly inertial propagation velocities, when the driving stress approaches the frictional strength characterizing the local minimum from above, and change their character when it is away from it. An approximate scaling theory quantitatively explains these observations. The derived pulse solutions also exhibit significant spatially-extended dissipation in excess of the edge-localized dissipation (the effective fracture energy) and an unconventional edge singularity. The relevance of our findings for available observations is discussed.

DOI: [10.1103/PhysRevE.107.L013001](https://doi.org/10.1103/PhysRevE.107.L013001)

Introduction. Compact spatiotemporal structures in driven dissipative systems, featuring long-range interactions, are of prime importance in a wide variety of physical systems [1,2]. A prominent example is frictional systems, composed of two deformable bodies in contact along a frictional interface, e.g., a geological fault in the earth's crust. When driven externally, interfacial slippage commences, accompanied by partial contact rupture and frictional strength reduction. This failure process—e.g., a propagating earthquake—is intrinsically inhomogeneous and often takes the form of spatially-compact, solitonic slip pulses [3–24]. In particular, it was shown that the duration of slip at a point on a fault is significantly shorter than the overall rupture duration, indicating its spatially-compact nature.

Slip pulses are self-healing in nature [5]. They feature significant strength reduction near their leading edge that invades a nearly quiescent, nonslipping interfacial state, but also strength recovery at their trailing edge, involving interfacial healing. Consequently, they feature a characteristic slipping length L over which nearly stationary contact is recovered. The trailing edge healing/restrengthening process is intimately related to the nonequilibrium nature of frictional interfaces, which undergo contact aging under nominally quiescent conditions [25–31]. Between the two edges, pulses feature finite slip velocities v . Numerous geophysical observations, laboratory experiments, and numerical simulations demonstrated that driven frictional systems can spontaneously generate long-lived, self-healing slip pulses [3–24]. Yet,

understanding the existence and properties of such self-healing pulses remains incomplete and challenging.

The problem involves a coarse-grained interfacial constitutive law, relating the frictional strength $\tau(v, \dots)$ to the slip velocity v and to a set of internal state fields represented by the ellipsis [28,30,32–34]. These describe the spatiotemporal structural state of the interface, corresponding to an evolving ensemble of contact asperities, and play the role of nonequilibrium order parameters. $\tau(v, \dots)$ is intrinsically nonlinear and accounts for significant energy dissipation. The nonlinear and dissipative interfacial constitutive law is coupled to the elastodynamic deformation of the bodies forming the interface, implying that distant parts of the interface are coupled by long-range spatiotemporal elastic forces. Finally, frictional systems are typically driven externally by far-field forces, e.g., a homogeneous shear stress τ_d .

Considering two large and identical linear elastic bodies in frictional contact, described by a spatial coordinate x , and focusing on objects propagating steadily at a velocity c_p , the interplay between the various physical ingredients discussed above is encapsulated in the following nonlinear integral equation [35]

$$\tau[v(\xi), \phi(\xi)] = \tau_d - \mu \mathcal{F}(\beta) \int_{-\infty}^{\infty} \frac{v(z)}{z - \xi} dz, \quad (1)$$

where $\xi = x - c_p t$ in a comoving coordinate (t is time). $\tau(v, \phi)$ is the frictional strength that depends, in addition to v , also on the field $\phi(\xi)$ that quantifies the amount of interfacial contact. The dynamics of $\phi(\xi)$ account for the competition between contact aging and slip-induced rejuvenation, to be discussed below.

$\tau(v, \phi)$ equals the interfacial shear stress, corresponding to the right hand side of Eq. (1). It is composed of the external

*These authors contributed equally to this work.

†eran.bouchbinder@weizmann.ac.il

driving shear stress τ_d and of a weighted integral over the slip velocity field $v(\xi)$, which represents the long-range elastodynamic interaction between different parts of the interface. μ is the shear modulus of the bodies and $\mathcal{F}(\beta)$ is a known function that accounts for material inertia, where $\beta \equiv c_p/c_s$ is the dimensionless propagation velocity and c_s is the shear wave speed of the bodies.

Steady state pulse solutions to Eq. (1) are those that satisfy the self-healing boundary conditions $v(\xi \rightarrow \pm\infty) \rightarrow 0$, i.e., solutions that feature a spatially compact $v(\xi)$. In this Letter, we numerically derive a family of such solutions for a generic and physically realistic interfacial constitutive law $\tau(v, \phi)$ [28,30,32–34,36]. We thoroughly analyze the properties of the emerging slip pulses and theoretically explain them. Finally, the relevance of our findings for available observations is briefly discussed.

The interfacial constitutive law. Eq. (1) constitutes a well defined problem once $\tau(v, \phi)$ and the evolution equation for $\phi(\xi)$ are specified. Over the last few decades, it has been established that the local contact area at frictional interfaces, which is typically orders of magnitude smaller than the nominal contact area, grows with the stationary contact ($v \rightarrow 0$) time t proportional to $\ln(1 + t/\phi_*)$, where ϕ_* is the contact aging onset time [25–31]. Contact aging leads to frictional strengthening and is described by an internal state field ϕ of time dimension, which identifies with t for $v \rightarrow 0$. Conversely, under steady sliding conditions at a slip velocity v , ϕ is proportional to $1/v$ [31], leading to contact rejuvenation and frictional weakening. The transition between the two regimes occurs over a characteristic slip distance D . These observations are accounted for by [28,30,34]

$$-\beta c_s \partial_\xi \phi(\xi) = 1 - \frac{|v(\xi)|\phi(\xi)}{D} \quad (2)$$

in terms of the comoving coordinate ξ .

The dimensionless frictional strength $f(v, \phi) \equiv \tau(v, \phi)/\sigma$, where σ is the normal stress that presses the two bodies together, incorporates the contact area ϕ dependence and an additional logarithmic rheological dependence on v [28,30,32–34,36], as presented in detail in [37]. Under steady sliding conditions, where Eq. (2) implies $\phi = D/v$, the steady sliding friction curve $\tau_{ss}(v)/\sigma = f(v, \phi = D/v)$ features an N shape, as demonstrated experimentally [36]. An example is presented in Fig. 1, where $\tau_{ss}(v)$ is velocity-strengthening ($d\tau_{ss}(v)/dv > 0$) at extremely small v , then it becomes logarithmically velocity-weakening ($d\tau_{ss}(v)/d \ln(v) = \text{const.} < 0$), and eventually logarithmically velocity-strengthening, beyond the minimum of the curve at (v_{\min}, τ_{\min}) .

A family of steady state pulse solutions. Eqs. (1) and (2) correspond to two space dimensions, i.e., translational invariance along the interface in the direction perpendicular to x (the out-of-plane direction) is assumed. Here, we focus on out-of-plane shear (mode-III symmetry), where $v(\xi)$ is perpendicular to the pulse propagation direction, and $\mathcal{F}_{\text{III}}(\beta) = \sqrt{1 - \beta^2}/(2\pi\beta c_s)$ (which vanishes as $\beta \rightarrow 1$). The counterpart in-plane (mode-II) solutions readily follow [37].

The self-healing boundary conditions, previously expressed as $v(\xi \rightarrow \pm\infty) \rightarrow 0$, take the form $v(\xi \rightarrow \pm\infty) = v_{\text{stick}}$, where v_{stick} is an extremely low slip velocity (cf. Fig. 1). Consequently, a pulse corresponds to a closed (homoclinic)

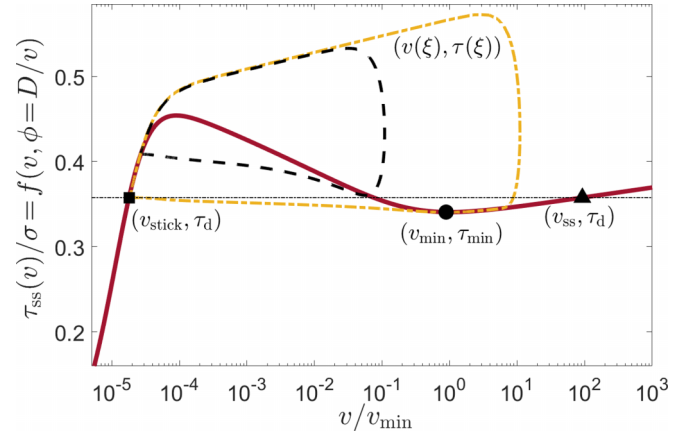


FIG. 1. τ_{ss} (solid line, in units of the normal stress σ) vs v/v_{\min} , featuring an N shape with a local minimum at (v_{\min}, τ_{\min}) (circle). For $\tau_d > \tau_{\min}$ (e.g., the horizontal dashed-dotted line), the equation $\tau_{ss}(v) = \tau_d$ features three solutions: the leftmost one (at extremely low v) is denoted by v_{stick} (square), the rightmost one is denoted by v_{ss} (triangle), and an intermediate one on the velocity-weakening branch (not marked). Two closed (homoclinic) orbits $(v(\xi), \tau(\xi))$, representing self-healing slip pulses, are added (dashed dotted line for $\tau_d/\tau_{\min} = 1.05$ and the dashed line for $\tau_d/\tau_{\min} = 1.20$).

orbit in the $(v(\xi), \tau(\xi))$ plane, which starts and ends at $(v_{\text{stick}}, \tau_d)$. Two such closed orbits, for two different τ_d values, are illustrated in Fig. 1.

We developed an accurate and robust numerical method to solve Eqs. (1) and (2) with the self-healing boundary conditions $v(\xi \rightarrow \pm\infty) = v_{\text{stick}}$, as detailed in [37]. The formulated problem admits a family of steady state self-healing pulse solutions as a function of τ_d , a few of which are presented in Fig. 2. In Fig. 2(a), $v(\xi)$ is presented, revealing a long healing tail at the trailing edge and a strong slip velocity amplification, by several orders of magnitude, near the leading edge.

In Fig. 2(b), the shear stress $\tau(\xi)$ —which equals the frictional strength—is presented. $\tau(\xi)$ attains a peak near the leading edge, which is significantly larger than the driving stress τ_d , attained far ahead of the pulse (to the right, full relaxation is not shown). Note also that the peak value itself is truncated in the figure). It then attains a minimum value, which decreases with τ_d , but appears to converge to a value τ_m that is close to τ_{\min} . Finally, $\tau(\xi)$ slowly approaches τ_d at the trailing edge, as the self-healing boundary condition is satisfied. The obtained solutions are highly accurate, featuring numerical convergence down to an error of $\mathcal{O}(10^{-15})$ and remarkable robustness with respect to the integration domain size [37].

The pulse length and propagation velocity: theoretical considerations and scaling relations. We first focus on the variation of the pulse properties with τ_d , most notably the pulse length L and the dimensionless pulse propagation velocity β . Note that the former does not appear in the problem formulation, but is rather defined *a posteriori*.

Under certain conditions, we expect L —operationally defined as the full width at half maximum of a logarithmic representation of $v(\xi)$ [37]—to diverge at a spacial driving stress τ_* . The physics here is that a steady state pulse may sometimes be envisioned as composed of a cracklike rupture

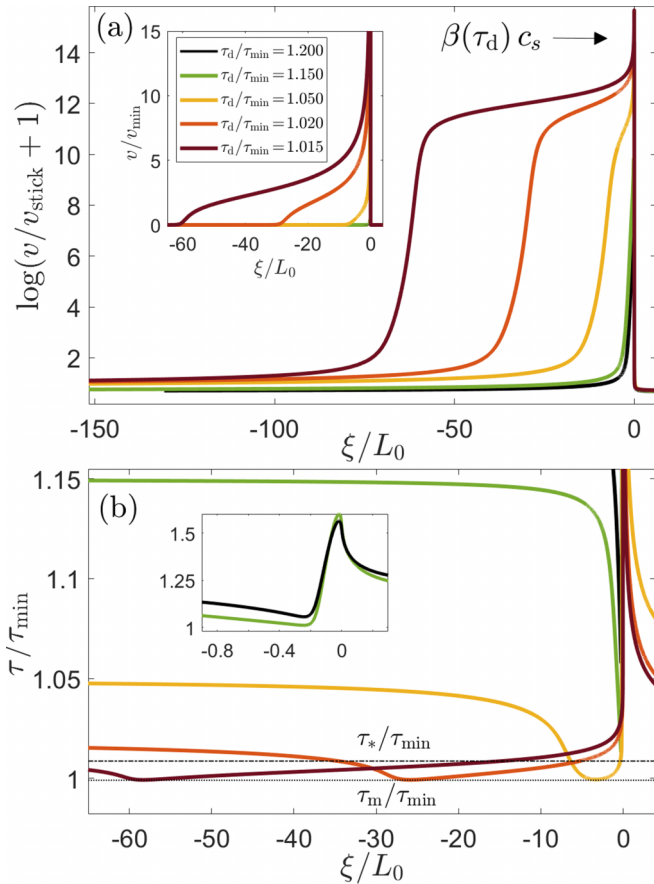


FIG. 2. (a) $\ln(v/v_{\text{stick}} + 1)$ vs ξ (normalized by the elastofrictional length L_0 [37]) for several pulse solutions traveling from left to right at a velocity $\beta(\tau_d)c_s$. τ_d for each curve is indicated in the legend in the inset, which presents the same results as the main panel, but in linear scale (v is normalized here by v_{min}). Note that the y axis in the inset is truncated and that the curves for the two largest τ_d 's are not clearly discernible. (b) τ/τ_{min} vs ξ/L_0 for the same solutions shown in panel (a). The minimal value τ_m of the three lowest τ_d curves (horizontal dotted line) and τ_* (horizontal dashed dotted line, see Eqs. (3) and (4) and the discussion therein) are marked. (inset) A zoom in on the two largest τ_d curves.

front—yet another prominent spatiotemporal mode of rupture of frictional systems [22,38–43]—and a healing front, both propagating in the same direction at the same velocity [20]. L is selected by the frictional interaction between these two fronts. Steady state cracklike fronts are related to the rightmost solution of $\tau_{\text{ss}}(v) = \tau_d$, denoted by v_{ss} in Fig. 1, where the stable fixed-point v_{ss} invades the v_{stick} fixed-point [20,40,44]. A healing front corresponds to the opposite/inverse situation, where the nearly quiescent state v_{stick} invades the sliding one, v_{ss} [20].

If isolated steady state cracklike and healing fronts exist at the same propagation velocity at $\tau_d = \tau_*$, a pulse of infinite extent ($L \rightarrow \infty$) can be constructed by simply superimposing these two noninteracting fronts. This physical picture was validated for frictional systems of small height [20] and is expected to remain valid for the infinite height systems considered here. It is relevant for pulses that probe the velocity-strengthening branch of the friction curve, where

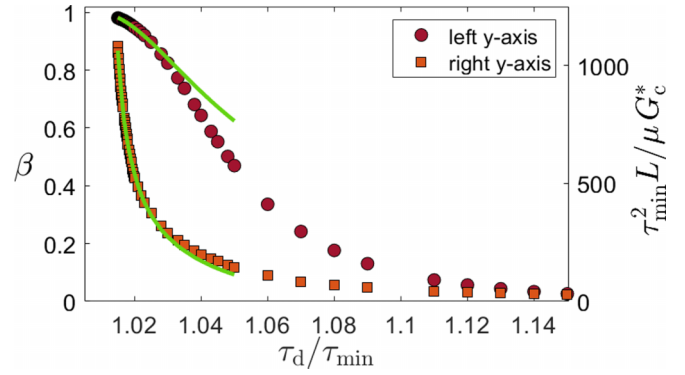


FIG. 3. $\beta(\tau_d)$ (left y axis) and $L(\tau_d)$ (right y axis, normalized by $\mu G_c^*/\tau_{\text{min}}^2$) of the obtained pulse solutions. We set $G_c^* = 0.65 \text{ J/m}^2$, previously obtained for the corresponding crack-like rupture [43]. The solid lines correspond to the theoretical predictions in Eqs. (3) and (4), see text for details.

v_{ss} resides. This is demonstrated by the closed $v - \tau$ orbit corresponding to $\tau_d/\tau_{\text{min}} = 1.05$ in Fig. 1. Consequently, we expect the physical picture of pulses being viewed at interacting cracklike and healing fronts to be valid for τ_d near τ_{min} , and L to diverge at $\tau_d = \tau_*$, which is very close to τ_{min} (below which v_{ss} does not exist anymore).

The existence of a minimum ($v_{\text{min}}, \tau_{\text{min}}$) of the friction curve and of v_{ss} are by no means necessary conditions for the existence of steady state pulses. These correspond to closed $v - \tau$ orbits that start and end at $(v_{\text{stick}}, \tau_d)$, and do not necessarily probe the minimum of the friction curve and the velocity-strengthening branch near it. This is expected to be the case for larger values of τ_d , away from the minimum τ_{min} , as is indeed demonstrated the closed $v - \tau$ orbit corresponding to $\tau_d/\tau_{\text{min}} = 1.2$ in Fig. 1. In this regime, we expect L to depend only mildly on τ_d . These expectations are verified in Fig. 3 (right y axis), where $L(\tau_d)$ is plotted and observed to strongly increase with decreasing τ_d , possibly consistent with a divergence as τ_{min} is approached, and to vary mildly with τ_d for larger values of τ_d . The corresponding results for $\beta(\tau_d)$ appear in Fig. 3 (left y axis), where β is observed to become strongly inertial ($\beta \rightarrow 1$) for small τ_d and quasistatic for larger values.

To understand the behavior of $L(\tau_d)$ and $\beta(\tau_d)$ with decreasing τ_d , near τ_{min} , we first note that the rate dependence of $\tau_{\text{ss}}(v)$ in Fig. 1 is predominantly logarithmic, i.e., rather weak. The recently developed theory of unconventional singularities of frictional rupture [45,46] predicts that for weak rate dependence the order of the edge singularity experienced by various fields differs from the classical $-\frac{1}{2}$ singularity of fracture mechanics only mildly [45]. With this in mind, we explore the possibility that *some physical quantities* approximately follow scaling relations inspired by classical pulse solutions featuring the classical $-\frac{1}{2}$ edge singularity.

Classical pulses with Coulomb (rate independent) friction [3] feature a length L , where inside the pulse $\tau(\xi) = \tau_{\text{res}}$ (the residual stress τ_{res} corresponds to a dynamic/sliding friction coefficient of magnitude τ_{res}/σ) and out of it $v(\xi) = 0$. The transition from static Coulomb friction out of the pulse to dynamic/sliding Coulomb friction inside is characterized by a finite fracture energy G_c , associated with a cohesive

zone slip of magnitude δ_c [3,47,48]. Formally, the boundary condition $\tau(\xi) = \tau_{\text{res}}$ inside the pulse is valid for slip δ satisfying $\delta > \delta_c$ (i.e., out of the cohesive zone). Solutions featuring a $-\frac{1}{2}$ power-law divergence near the leading edge at ξ_p , and no divergence (but a discontinuous derivative) at the trailing edge, take the form $v(\xi) = v_0 \sqrt{(L + \xi_p - \xi)/(\xi - \xi_p)}$ [3]. The slip velocity at the middle of the pulse, v_0 , satisfies $2c_s \beta = v_0 \mu \sqrt{1 - \beta^2} (\tau_d - \tau_{\text{res}})^{-1}$ and L satisfies $\pi L = \mu G_c \sqrt{1 - \beta^2} (\tau_d - \tau_{\text{res}})^{-2}$ [3].

These relations do *not* constitute a complete solution, as they feature three unknowns— β , L and v_0 —and only two constraints. However, as our rate-and-state pulses solutions for τ_d near τ_{min} involve a characteristic slip velocity v_{min} (absent in the classical problem), we identify v_0 with $a_v v_{\text{min}}$, with a_v of $\mathcal{O}(1)$. Moreover, we identify the stress τ_{res} with τ_* —the hypothesized stress at which L diverges—expected to be very close to τ_{min} . Finally, as we expect our pulses to feature an effective fracture energy G_c that is similar to their cracklike counterparts, we set $G_c = a_G G_c^*$, with a_G of $\mathcal{O}(1)$ and G_c^* is the known cracklike value [43].

Taken together, we obtain

$$\beta = a_v \left(\frac{v_{\text{min}} \mu}{2\tau_{\text{min}} c_s} \right) \frac{\sqrt{1 - \beta^2}}{(\tau_d/\tau_{\text{min}} - \tilde{\tau}_*)}, \quad (3)$$

$$\tilde{L} \equiv \frac{\tau_{\text{min}}^2 L}{\mu G_c^*} = a_G \frac{\sqrt{1 - \beta^2}}{\pi (\tau_d/\tau_{\text{min}} - \tilde{\tau}_*)^2}, \quad (4)$$

where \tilde{L} is the nondimensionalized L and $\tilde{\tau}_* \equiv \tau_*/\tau_{\text{min}}$. These predictions are quantitatively verified in Fig. 3 (solid lines), with $\tilde{\tau}_* = 1.0087$, $a_v = 1.15$ and $a_G = 0.69$ [note that τ_* is distinct from τ_m , cf. Fig. 2(b)]. We thus conclude that the approximate scaling relations in Eqs. (3) and (4), together with the physical concepts and ideas incorporated into them, properly describe our steady state pulses for τ_d near τ_* .

Energy dissipation and unconventional edge singularity.

The above analysis indicates that our pulses for τ_d close to τ_* (but not away from it) resemble in some respects classical pulses with Coulomb (rate independent) friction. Yet, on general grounds, we expect the intrinsic rate (and state) dependence of friction to make qualitative differences. To highlight this, we consider the slip pulse energy budget, in particular the local breakdown energy $\bar{G}(\delta)$ [22]

$$\bar{G}(\delta) = \int_0^\delta [\tau(\delta') - \tau_m] d\delta'. \quad (5)$$

Here $\delta(r) = (\beta c_s)^{-1} \int_0^r [v(s) - v_{\text{stick}}] ds$ (s increases from the leading edge backward) is the slip accumulated by the pulse and τ_m is the minimum of $\tau(\xi)$ for τ_d close to τ_* , cf. Fig. 2(b).

For classical pulses, we have $\tau_m = \tau_{\text{res}}$ and $\bar{G}(\delta) = G_c$ for $\delta > \delta_c$ (recall that for classical pulses $\tau(\delta) = \tau_{\text{res}}$ for $\delta > \delta_c$), independently of the driving stress τ_d , and hence also of β and L . In Fig. 4, we present $\bar{G}(\delta)$ of our solutions for τ_d close to τ_* . It is observed that all curves overlap at small δ , indicating the existence of a well defined effective fracture energy G_c (and of δ_c [37]), corresponding to edge-localized dissipation. The various curves fan out at $G_c \simeq 0.6 \text{ J/m}^2$, marked in Fig. 4 (in quantitative agreement with their cracklike counterparts, see caption of Fig. 3 and [43]). For larger δ 's, the curves significantly deviate from G_c (reaching values as high as $\sim 4G_c$,

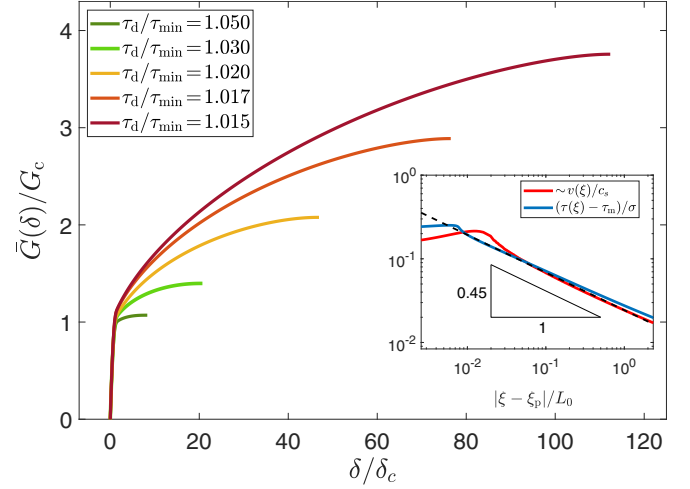


FIG. 4. $\bar{G}(\delta)$ of Eq. (5), normalized by $G_c = 0.6 \text{ J/m}^2$, vs slip δ normalized by $\delta_c = 3.7 \times 10^{-6} \text{ m}$, for τ_d 's as indicated in the legend. The values of G_c and δ_c are extracted from the collapse of all curves at small δ , as shown in Fig. S4 of [37]. Indeed, the different curves fan out at $\bar{G}(\delta_c) \simeq G_c$. (inset) A singularity analysis of the near leading-edge fields, see legend and [37]. The singularity order of the fields is $\simeq -0.45$ (dashed line and scaling triangle), see text for additional details.

attained for the smallest τ_d considered), revealing excess dissipation that is distributed over the pulse length, which is entirely absent in classical pulses.

A recently developed theory [45,46], mentioned above, showed that such spatially-extended excess dissipation is associated with the existence of unconventional singularities, i.e., with near leading edge fields featuring a singularity order different from the classical $-\frac{1}{2}$ one. For the logarithmic rate dependence in Fig. 1, the singularity order deviation is predicted to be rather small, but the excess dissipation is large and increases with L . To test these predictions, we simultaneously fitted $v(\xi)$ behind the pulse leading edge (i.e., $\xi < \xi_p$ in Fig. 2) to $v(\xi) \sim (\xi_p - \xi)^\zeta$ and $\tau(\xi)$ ahead of the leading edge (i.e., $\xi > \xi_p$ in Fig. 2) to $\tau(\xi) - \tau_m \sim (\xi - \xi_p)^\zeta$, for the smallest τ_d considered (largest L). The results are shown in the inset of Fig. 4, where the singularity order is $\zeta \simeq -0.45$, which indeed deviates from $-\frac{1}{2}$, as predicted. These results clearly demonstrate that rate-and-state pulses reveal qualitative differences compared to their classical counterparts.

Summary and outlook. We derived a family of steady state self-healing (solitonic) slip pulses in frictional systems for a realistic, experimentally supported, interfacial constitutive law. The physical properties of the pulses have been thoroughly analyzed and theoretically explained. These results are of general importance for understanding spatiotemporal structures in driven nonlinear dissipative systems, featuring long-range interactions, and in particular for understanding the failure dynamics of frictional systems. For example, they can lead to improved source time functions for seismic inversion [24].

In the latter context, it is established that elasto-frictional instabilities—where large amounts of stored elastic energy are abruptly released—can spontaneously trigger long-lived pulse-like rupture (i.e., propagating long distances without

appreciably changing its properties). How do such dynamically generated long-lived pulse-like ruptures relate to the steady state pulse solutions derived here? To fully address this question, one should first determine the dynamic stability of the derived solutions (when steady state conditions are not imposed), which is currently unknown. There are, however, some indications that these solutions might be dynamically unstable [5,20,21].

If true, then one can speculate that the growth rate of the dynamic instability is small and hence while steady state pulse

solutions do not constitute a stable attractor (in the dynamical systems sense), a frictional system can nonetheless reside for rather long times near it. Addressing these important questions requires dynamical calculations, which is a challenge for future investigations.

Acknowledgments. This work has been supported by the Israel Science Foundation (Grant No. 1085/20). E.B. acknowledges support from the Ben May Center for Chemical Theory and Computation and the Harold Perlman Family.

-
- [1] A. C. Newell, *Solitons in Mathematics and Physics* (SIAM, 1985)
- [2] T. Dauxois and M. Peyrard, *Physics of Solitons* (Cambridge University Press, 2006).
- [3] L. B. Freund, The mechanics of dynamic shear crack propagation, *J. Geophys. Res.* **84**, 2199 (1979).
- [4] T. H. Heaton, Evidence for and implications of self-healing pulses of slip in earthquake rupture, *Phys. Earth Planet. Inter.* **64**, 1 (1990).
- [5] G. Perrin, J. R. Rice, and G. Zheng, Self-healing slip pulse on a frictional surface, *J. Mech. Phys. Solids* **43**, 1461 (1995).
- [6] G. C. Beroza and T. Mikumo, Short slip duration in dynamic rupture in the presence of heterogeneous fault properties, *J. Geophys. Res.* **101**, 22449 (1996).
- [7] N. M. Beeler and T. E. Tullis, Self-healing slip pulses in dynamic rupture models due to velocity-dependent strength, *Bull. Seismol. Soc. Am.* **86**, 1130 (1996).
- [8] A. Cochard and R. Madariaga, Complexity of seismicity due to highly rate-dependent friction, *J. Geophys. Res.* **101**, 25321 (1996).
- [9] D. J. Andrews and Y. Ben-Zion, Wrinkle-like slip pulse on a fault between different materials, *J. Geophys. Res.* **102**, 553 (1997).
- [10] G. Zheng and J. R. Rice, Conditions under which velocity-weakening friction allows a self-healing versus a cracklike mode of rupture, *Bull. Seismol. Soc. Am.* **88**, 1466 (1998).
- [11] S. B. Nielsen, J. M. Carlson, and K. B. Olsen, Influence of friction and fault geometry on earthquake rupture, *J. Geophys. Res.* **105**, 6069 (2000).
- [12] S. Nielsen and R. Madariaga, On the Self-Healing Fracture Mode, *Bull. Seismol. Soc. Am.* **93**, 2375 (2003).
- [13] E. A. Brener, S. V. Malinin, and V. I. Marchenko, Fracture and friction: Stick-slip motion, *Eur. Phys. J. E* **17**, 101 (2005).
- [14] Z. Shi, Y. Ben-Zion, and A. Needleman, Properties of dynamic rupture and energy partition in a solid with a frictional interface, *J. Mech. Phys. Solids* **56**, 5 (2008).
- [15] A. M. Rubin and J.-P. Ampuero, Self-similar slip pulses during rate-and-state earthquake nucleation, *J. Geophys. Res.* **114**, D11305 (2009).
- [16] D. I. Garagash, Seismic and aseismic slip pulses driven by thermal pressurization of pore fluid, *J. Geophys. Res.* **117**, B04314 (2012).
- [17] A.-A. Gabriel, J.-P. Ampuero, L. A. Dalguer, and P. M. Mai, The transition of dynamic rupture styles in elastic media under velocity-weakening friction, *J. Geophys. Res.* **117**, B09311 (2012).
- [18] T. Putelat, J. H. Dawes, and A. R. Champneys, A phase-plane analysis of localized frictional waves, *Proc. R. Soc. A Math. Phys. Eng. Sci.* **473**, 20160606 (2017).
- [19] S. Michel, J.-P. Avouac, N. Lapusta, and J. Jiang, Pulse-like partial ruptures and high-frequency radiation at creeping-locked transition during megathrust earthquakes, *Geophys. Res. Lett.* **44**, 8345 (2017).
- [20] E. A. Brener, M. Aldam, F. Barras, J.-F. Molinari, and E. Bouchbinder, Unstable Slip Pulses and Earthquake Nucleation as a Nonequilibrium First-Order Phase Transition, *Phys. Rev. Lett.* **121**, 234302 (2018).
- [21] N. Brantut, D. I. Garagash, and H. Noda, Stability of pulse-like earthquake ruptures, *J. Geophys. Res. Solid Earth* **124**, 8998 (2019).
- [22] V. Lambert, N. Lapusta, and S. Perry, Propagation of large earthquakes as self-healing pulses or mild cracks, *Nature (London)* **591**, 252 (2021).
- [23] T. Roch, E. A. Brener, J.-F. Molinari, and E. Bouchbinder, Velocity-driven frictional sliding: Coarsening and steady-state pulses, *J. Mech. Phys. Solids* **158**, 104607 (2022).
- [24] J. Galetzka, D. Melgar, J. F. Genrich, J. Geng, S. Owen, E. O. Lindsey, X. Xu, Y. Bock, J.-P. Avouac, L. B. Adhikari *et al.*, Slip pulse and resonance of the Kathmandu basin during the 2015 Gorkha earthquake, Nepal, *Science* **349**, 1091 (2015).
- [25] J. H. Dieterich, Time-dependent friction and the mechanics of stick-slip, *Pure Appl. Geophys.* **116**, 790 (1978).
- [26] J. H. Dieterich and B. D. Kilgore, Direct observation of frictional contacts: New insights for state-dependent properties, *Pure Appl. Geophys.* **143**, 283 (1994).
- [27] N. M. Beeler, T. E. Tullis, and J. D. Weeks, The roles of time and displacement in the evolution effect in rock friction, *Geophys. Res. Lett.* **21**, 1987 (1994).
- [28] C. Marone, Laboratory-derived friction laws and their application to seismic faulting, *Annu. Rev. Earth Planet. Sci.* **26**, 643 (1998).
- [29] P. Berthoud, T. Baumberger, C. G'Sell, and J.-M. Hiver, Physical analysis of the state- and rate-dependent friction law: Static friction, *Phys. Rev. B* **59**, 14313 (1999).
- [30] T. Baumberger and C. Caroli, Solid friction from stick-slip down to pinning and aging, *Adv. Phys.* **55**, 279 (2006).
- [31] O. Ben-David, S. M. Rubinstein, and J. Fineberg, Slip-stick and the evolution of frictional strength, *Nature (London)* **463**, 76 (2010).

- [32] J. H. Dieterich, Modeling of rock friction: 2. Simulation of preseismic slip, *J. Geophys. Res.* **84**, 2169 (1979).
- [33] A. L. Ruina, Slip instability and state variable friction laws, *J. Geophys. Res.* **88**, 10359 (1983).
- [34] M. Nakatani, Conceptual and physical clarification of rate and state friction: Frictional sliding as a thermally activated rheology, *J. Geophys. Res.* **106**, 13347 (2001).
- [35] J. Weertman, Unstable slippage across a fault that separates elastic media of different elastic constants, *J. Geophys. Res.* **85**, 1455 (1980).
- [36] Y. Bar-Sinai, R. Spatschek, E. A. Brener, and E. Bouchbinder, On the velocity-strengthening behavior of dry friction, *J. Geophys. Res. Solid Earth* **119**, 1738 (2014).
- [37] See Supplemental Material at <http://link.aps.org/supplemental/10.1103/PhysRevE.107.L013001> for additional information, which includes Refs. [5,16,20,21,28,30,32–34,36,43–46,49–53].
- [38] Y. Ben-Zion, Dynamic ruptures in recent models of earthquake faults, *J. Mech. Phys. Solids* **49**, 2209 (2001).
- [39] C. H. Scholz, *The Mechanics of Earthquakes and Faulting* (Cambridge university press, 2002).
- [40] Y. Bar Sinai, E. A. Brener, and E. Bouchbinder, Slow rupture of frictional interfaces, *Geophys. Res. Lett.* **39**, L03308 (2012).
- [41] I. Svetlizky, E. Bayart, and J. Fineberg, Brittle Fracture Theory Describes the Onset of Frictional Motion, *Annu. Rev. Condens. Matter Phys.* **10**, 031218 (2019).
- [42] F. Barras, M. Aldam, T. Roch, E. A. Brener, E. Bouchbinder, and J.-F. Molinari, Emergence of Cracklike Behavior of Frictional Rupture: The Origin of Stress Drops, *Phys. Rev. X* **9**, 041043 (2019).
- [43] F. Barras, M. Aldam, T. Roch, E. A. Brener, E. Bouchbinder, and J.-F. Molinari, The emergence of cracklike behavior of frictional rupture: Edge singularity and energy balance, *Earth Planet. Sci. Lett.* **531**, 115978 (2020).
- [44] Y. Bar-Sinai, M. Aldam, R. Spatschek, E. A. Brener, and E. Bouchbinder, Spatiotemporal Dynamics of Frictional Systems: The Interplay of Interfacial Friction and Bulk Elasticity, *Lubricants* **7**, 91 (2019).
- [45] E. A. Brener and E. Bouchbinder, Unconventional singularities and energy balance in frictional rupture, *Nat. Commun.* **12**, 2585 (2021).
- [46] E. A. Brener and E. Bouchbinder, Theory of unconventional singularities of frictional shear cracks, *J. Mech. Phys. Solids* **153**, 104466 (2021).
- [47] A. C. Palmer and J. R. Rice, The Growth of Slip Surfaces in the Progressive Failure of Over-Consolidated Clay, *Proc. R. Soc. A* **332**, 527 (1973).
- [48] Y. Ida, Cohesive force across the tip of a longitudinal-shear crack and Griffith's specific surface energy, *J. Geophys. Res.* **77**, 3796 (1972).
- [49] Y. Estrin and Y. Bréchet, On a model of frictional sliding, *Pure Appl. Geophys.* **147**, 745 (1996).
- [50] MATLAB, *version 9.9.0 (R2020b)* (The MathWorks Inc., Natick, Massachusetts, 2020).
- [51] K. B. Broberg, *Cracks and Fracture* (Elsevier, 1999).
- [52] M. Cocco and A. Bizzarri, On the slip-weakening behavior of rate- and state dependent constitutive laws, *Geophys. Res. Lett.* **29**, 1516 (2002).
- [53] A. Bizzarri and M. Cocco, Slip-weakening behavior during the propagation of dynamic ruptures obeying rate- and state-dependent friction laws, *J. Geophys. Res.* **108**, 2373 (2003).